Roles of Proximal Ligand in Heme Proteins: Replacement of Proximal Histidine of Human Myoglobin with Cysteine and Tyrosine by Site-Directed Mutagenesis as Models for P-450, Chloroperoxidase, and Catalase†

Shin-ichi Adachi,‡ Shingo Nagano, Koichiro Ishimori, Yoshihito Watanabe, and Isao Morishima*

Division of Molecular Engineering, Graduate School of Engineering, Kyoto University, Kyoto 606-01, Japan

Tsuyoshi Egawa§ and Teizo Kitagawa

The Institute for Molecular Science, Okazaki National Research Institutes, Myodaiji, Okazaki 444, Japan

Ryu Makino

Himeji Institute of Technology, Akō-gun, Hyogo 678-12, Japan

Received June 10, 1992; Revised Manuscript Received September 23, 1992

ABSTRACT: Histidine-93(F8) in human myoglobin (Mb), which is the proximal ligand of the heme iron, has been replaced with cysteine or tyrosine by site-directed mutagenesis. The resultant proximal cysteine and tyrosine mutant Mbs (H93C and H93Y Mbs, respectively) exhibit the altered axial ligation analogous to P-450, chloroperoxidase, and catalase. Coordination of cysteine or tyrosine to the ferric heme iron is confirmed by spectroscopic measurements including electronic absorption, hyperfine-shifted ^{1}H-NMR, EPR, resonance Raman spectroscopies, and redox potential measurements of ferric/ferrous couple. H93C Mb is five-coordinate ferric high-spin with the proximal cysteine. H93Y Mb bearing the proximal tyrosine ligated to the iron is also in a ferric high-spin, five-coordinate state. The reactions of the mutants with cumene hydroperoxide show that the thiolate ligand enhances heterolytic O–O bond cleavage of the oxidant, while the phenolate ligand hardly affects the heterolysis/homolysis ratio for O–O bond scission in comparison with wild-type Mb. Monooxygenase activities such as epoxidation of styrene and N-demethylation of *N*,*N*-dimethylaniline, and catalase activity (dismutation of hydrogen peroxide) by wild-type Mb and the mutants, are examined by using H_2O_2. The increase of the catalytic activities by the mutation was, at most, 5-fold in the epoxidation reaction.

Oxo–ferryl porphyrin π-cation radical species ($Por^{+\bullet}Fe(IV)=O$, compound I) have been postulated to be highly active reaction intermediates responsible for the catalytic reactions of heme enzymes such as P-450, peroxidase, and catalase (Ortiz de Montellano, 1986; White & Coon, 1980; Dunford & Stillman, 1976; Hewson & Hager, 1979; Dolphin et al., 1971). In fact, the formation of compound I has been observed in various heme enzymes (Dunford, 1982; Chance, 1943, 1949; George, 1953; Maguire et al., 1971; Palcic et al., 1980; Harrison et al., 1980; Schonbaum & Chance, 1976; Roberts et al., 1981a,b; Penner-Hahn et al., 1983; Chance et al., 1984; La Mar et al., 1981; Schulz, 1979, 1984; Browett et al., 1983). Compound I is readily observed by utilizing the reactions of hydroperoxides (ROOH) or their equivalents with ferric heme proteins or model porphyrin complexes (Dunford, 1982; Chance, 1943, 1949; George, 1953; Maguire et al., 1971; Palcic et al., 1980; Harrison et al., 1980; Schonbaum & Chance, 1976; Roberts et al., 1981a,b; Penner-Hahn et al., 1983; Chance et al., 1984; La Mar et al., 1981; Schulz, 1979, 1984; Browett et al., 1983; Morishima et al., 1983, 1984, 1986; Groves et al., 1981; Groves & Watanabe, 1988; Yamaguchi et al., 1992). The oxygen atom transfer of hydroperoxide in eq 1 has been shown to occur by heterolytic O–O bond cleavage to form compound I. On the other hand, homolytic scission of the O–O bond provides oxo–ferryl species ($PorFe(IV)=O$, compound II) as shown in eq 2.

$$PorFe^{III} + ROOH \rightarrow Por^{+\bullet}Fe^{IV}=O + ROH \quad (1)$$

$$PorFe^{III} + ROOH \rightarrow PorFe^{IV}=O + RO^{\bullet} + H^{+} \quad (2)$$

Biological manipulation of oxidizing equivalent as compound I against a Fenton type free radical process has been attributed to the utilization of an anionic axial ligand of the heme iron (Morrison & Schonbaum, 1976; Peisach, 1975; Dawson et al., 1976; Dawson & Sono, 1987; Dawson, 1988); i.e., Cys^- in P-450 and chloroperoxidase (CPO), Tyr^- in catalase, and $His(Im^-)$ or $His(Im\text{-}H\cdots X)$ in horseradish peroxidase (HRP) and cytochrome *c* peroxidase (CCP). In the case of P-450, Dawson and co-workers have claimed a role of the thiolate ligation to the heme iron as a strong electron donor to facilitate heterolytic O–O bond cleavage (Dawson et al., 1976; Dawson & Sono, 1987; Dawson, 1988). In spite of untiring efforts to clarify the role of the anionic axial ligands of heme enzymes on the O–O bond cleavage reaction, it remains obscure and open for further studies.

Recent in vitro mutagenesis techniques have enabled us to genetically engineer myoglobin (Mb) by employing the resultant high-level expression system in *Escherichia coli*

† This study was supported by a Grant-in-Aid for Scientific Research on Priority Areas (03241103) to I.M.

* To whom correspondence should be addressed; FAX (075) 751-7611.

‡ Present address: Photon Factory, National Institute for High Energy Physics, Tsukuba, Ibaraki 305, Japan.

§ Present address: Department of Biochemistry, School of Medicine, Keio University, Tokyo 160, Japan.

0006-2960/93/0432-241$04.00/0

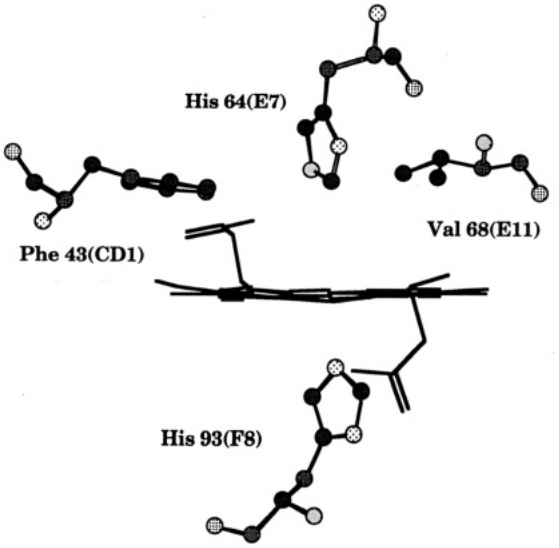

FIGURE 1: Heme environmental structure of myoglobin. The heme and some selected myoglobin residues including proximal His93(F8) are shown.

(Varadarajan et al., 1985; Springer & Sligar, 1987). Now, we are able to replace the axial ligand [His93(F8) (Figure 1)] of Mb with Cys or Tyr by site-directed mutagenesis as models for heme enzymes and examine roles of the axial ligand on the O–O bond cleavage reaction. Recently, Egeberg et al. (1990) reported the replacement of proximal His of recombinant sperm whale Mb to Tyr by site-directed mutagenesis. While they showed the spectroscopic properties of the mutant being similar to natural mutants of hemoglobin (Hb M Iwate or Hb M Hyde Park) and catalase, effects of the ligand replacement on its reactions with oxidants have not been reported. Here we report the preparation, characterization, reactions with peroxides, and catalytic activities of the novel human Mb mutants whose proximal His93(F8) are substituted with Cys or Tyr (H93C and H93Y Mbs, respectively).

EXPERIMENTAL PROCEDURES

Site-Directed Mutagenesis, Protein Preparation, and Purification. The original expression vector of human Mb gene, pMb3 (pLcIIFXMb), is a gift from Varadarajan and Boxer (Varadarajan et al., 1985). The procedures for site-directed mutagenesis and DNA sequencing are described elsewhere (Adachi et al., 1991). Protein preparation and purification were performed according to the method described by Varadarajan et al., (1989a). QY13 (*F⁻ lac$_{am}$trp$_{am}$B B′ bio-256 N⁺ cI857 ΔH Sm^r recA*) was used as a host strain. QY13 harboring pMb3 was grown at 30 °C in 2 × TY medium (10 g of tryptone, 10 g of yeast extract, 5 g of NaCl, and 1.6 mL of 2 N NaOH per liter) in the presence of ampicillin (50 μg/mL). When the optical density at 600 nm of the culture reached 1.0, the temperature was quickly raised and maintained at 42 °C for 15 min, followed by further incubation at 37 °C for 7–8 h. The cells were harvested and frozen in a deep freezer. The cells were thawed and suspended in 80 mL of 50 mM Tris-HCl buffer (pH 8.0) including 25% sucrose (w/v)/1 mM EDTA and lysed by addition of lysozyme (200 mg). Then, $MgCl_2$, $MnCl_2$, and DNase I were added to final concentrations of 10 mM, 1 mM, and 10 μg/mL, respectively. After 30-min incubation, a 200-mL solution of 0.2 M NaCl/1% deoxycholic acid/1.6% Nonidet P-40 (v/v)/20 mM Tris-HCl (pH 7.5)/2 mM EDTA was added to the lysate, which was then centrifuged at 7000*g* for 10 min. The pellet was suspended in 0.5% Triton X-100/1 mM EDTA and centrifuged. This procedure was repeated until a tight pellet was obtained. The protein pellet was finally dissolved in 8 M urea/25 mM Tris-HCl (pH 8)/1 mM EDTA. The solubilized denatured protein solution was diluted 16-fold by 10 mM Tris-HCl (pH 9.5). To the supernatant at 4 °C was added 1.1 equiv of a 2 mM solution of protohemin in dimethylformamide, and the solution was left to stand for 15 min at 4 °C. The reconstituted fusion protein was digested with 50 μg/mL trypsin (type III, Sigma) at 20 °C. After 2-h incubation, the pH of the solution was raised to 9.2, and the protein was loaded onto a 5- × 10-cm DE-52 column (Whatman) that had been equilibrated with 10 mM Tris-HCl, pH 9.5, at 4 °C. At this stage the fusion protein was digested by trypsin to an intermediate product of molecular weight approximately 18 000 that probably results from cleavage of the fusion protein at Lys ten amino acids upstream from the end of the FX_a site (Nagai & Thøgersen, 1984). This cleavage product was eluted with 50 mM Tris-HCl, pH 7.5, and concentrated with Amicon YM5 membrane. Trypsin was added to a final concentration of 50 μg/mL, and the intermediate was digested for 3 h at 20 °C to give the desired product. The protein was submitted to a Sephadex G-25 column equilibrated with 10 mM Tris-HCl, pH 9.0, for buffer exchange and loaded onto a DE-52 column, eluted with 50 mM Tris-HCl, pH 7.5. SDS–polyacrylamide gel electrophoresis was utilized to check the purity of the final sample which consisted of a single band.

Spectroscopy. All spectroscopic measurements were performed in 50 mM sodium phosphate buffer, pH 7.0, unless stated. Electronic absorption spectra of purified proteins were recorded on a Hitachi U-3210 UV/visible spectrophotometer equipped with a cell holder for low-temperature measurement. Concentration of the samples was 10 μM.

Electron paramagnetic resonance (EPR) measurements were carried out at X-band (9.35-GHz) microwave frequency with 100-kHz field modulation by use of a Varian X-band cavity at 4.2 K. Concentration of the samples was 0.5 mM.

Hyperfine-shifted ^{1}H-NMR spectra were recorded at 300 MHz on a Nicolet NT-300 spectrometer equipped with a 1280 computer system. For recording of the hyperfine-shifted ^{1}H-NMR spectra, 30–50K transients were accumulated to obtain the Fourier transformed spectra with 4K data points and a 6.6-μs 90° pulse. Chemical shifts are referenced to H_2O, and downfield shifts are given a positive sign. Concentration of the samples for NMR measurements was 1 mM, and experiments were performed at 23 °C.

Resonance Raman scattering was excited at 363.8 or 488.0 nm generated by an Ar^+ ion laser (Spectra Physics, 2045), 441.6 nm of a He/Cd laser (Kinmon Electronics, CDR80SG), or 420 nm generated through a dye laser (Spectra Physics, 375B) by exciting stilbene-420 with the 363.8–365.1-nm lines of an Ar^+ ion laser. Detection was performed by an intensified silicon photodiode array (PAR 1421-HQ) attached to a triple spectrograph (Spex 1877 0.6-m triple spectrometer), or by a JEOL-400D Raman spectrometer equipped with a cooled HTV-943-02 photomultiplier. The frequencies of the Raman spectrometer were calibrated with indene or ethanol for each measurement. The concentrations of samples were 30, 30, 50, and 200 μM for the excitations at 420, 441.6, 363.8, and 488.0 nm, respectively.

Measurements of Monooxygenase and Catalase Activities. A solution of ferric wild-type or mutant Mb (50 μM) and styrene (15 mM) in 50 mM sodium phosphate buffer (pH 7.0) was preincubated at 30 °C for 20 min. Incubation of a 1-mL solution was routinely employed twice for each experimental point. A preincubated solution of hydrogen peroxide

in 50 mM phosphate buffer (final concentration 1 mM) was added to initiate the reaction, and the mixture was incubated at 30 °C for 2 min. Cumyl alcohol (243 μg/mL) was added as an internal standard at the end of the incubation period to quantitate product formation. The incubation mixture was then extracted with 5 mL of diethyl ether. The extract was dried over anhydrous sodium sulfate. After evaporation of most of ether, the metabolites were determined by GLC.

GLC analyses were performed on a Shimadzu GC-14A fitted with a Shimadzu CBP1 (25-m) capillary column. HPLC analyses were carried out on a Waters 600 equipped with Waters 741 data module. Chiral HPLC column (CHIRALCEL OJ; DAICEL Chemical Industries, Ltd.) was used for the determination of the absolute chirality of styrene oxide with 0.5% 2-propanol in hexane. The eluent was monitored at 220 nm with a Waters Lambda-Max Model 481 LC spectrophotometer. Chirality of styrene oxide was determined by comparison with pure (*R*)-styrene oxide (Nippon Mining Co., Ltd.).

N-Demethylation of *N*,*N*-dimethylaniline was performed under the same reaction conditions. The reaction mixture was quenched by addition of 1 mL of 10% trichloroacetic acid, and protein precipitate was removed by centrifugation (15K rpm × 5 min). To the supernatant was added 0.5 mL of cooled Nash reagent (4 M ammonium acetate and 40 mM 2,4-pentanedione), and the solution was incubated for 30 min at 60 °C. After the incubation, the amount of formaldehyde formed was determined by the absorbance of the solution at 415 nm.

Dismutation of hydrogen peroxide was examined by the oxygen evolution monitored by an oxygen electrode (YSI 5331 probe). To a solution of ferric Mb (30 μM) was added hydrogen peroxide (1 mM final concentration), and incubation was terminated when the steep rise of oxygen evolution was stopped. The amount of evoluted oxygen and hence consumed hydrogen peroxide was determined with reference to that of dissolved oxygen in the buffer at 20 °C.

Reaction with Cumene Hydroperoxide. A protein solution (10 μM in 2 mL of 50 mM sodium phosphate buffer, pH 7.0) was incubated with cumene hydroperoxide (240 μM) at 20 °C. During the incubation, aliquots of the solution (5 μL) were directly loaded on HPLC. Reverse-phase HPLC (Waters μBondasphere 5 μm CN-100 Å) was employed to determine the reaction products, which were eluted at 0.6 mL/min with 70% H_2O/30% methanol. The eluent was monitored at 210 nm, and assignment of the components was based on the retention time of authentic samples.

RESULTS

Electronic Absorption Spectroscopy. Electronic absorption spectra of the ferric forms of wild-type and mutant Mbs have been reported and discussed previously (Adachi et al., 1991). Figures 2 and 3 exhibit electronic absorption spectra of ferric, ferrous, and carbon monoxy ($Fe^{2+}CO$) forms of the mutants. In contrast to the electronic absorption spectra of the ferric forms of the mutants, spectra of ferrous H93C and H93Y Mbs are very similar to that of wild-type Mb (Antonini & Brunori, 1971). Upon reduction of H93C and H93Y Mbs with sodium dithionite under CO atmosphere, the CO complexes of the mutants were obtained as stable species. Since the absorption spectrum of the CO complex of H93C Mb shows a similar spectrum to that of wild-type Mb (Soret band; λ_{max} = 420 nm), it is unlikely that the proximal thiolate remains ligated to the ferrous iron. Due to rapid autoxidation

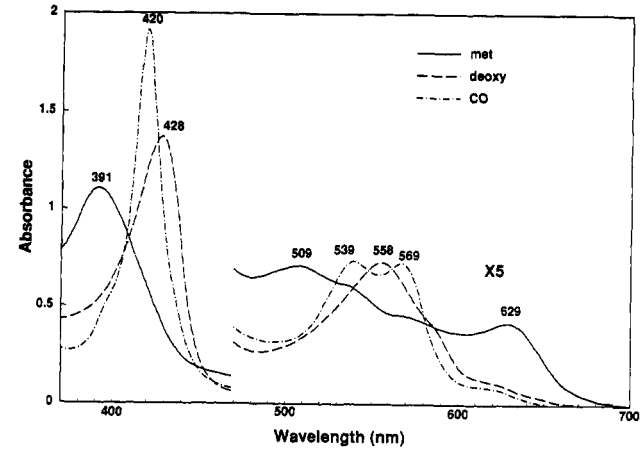

FIGURE 2: Electronic absorption spectra of ferric high-spin, ferrous high-spin, and carbonmonoxy forms of human H93C Mb in 50 mM sodium phosphate buffer at pH 7.0 and 20 °C. The concentration of the sample is 10 μM.

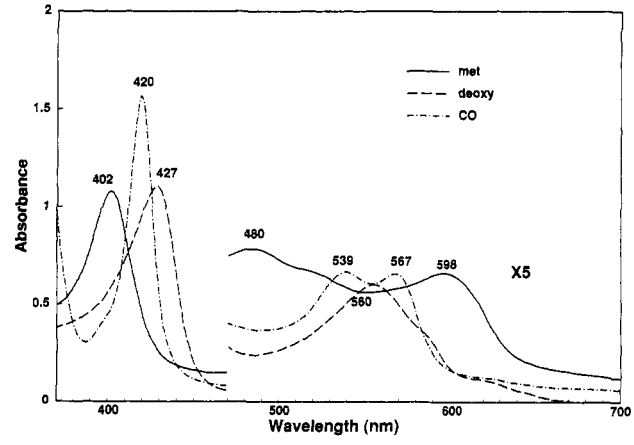

FIGURE 3: Electronic absorption spectra of ferric high-spin, ferrous high-spin, and carbonmonoxy forms of human H93Y Mb. Conditions of samples are the same as in Figure 2.

of oxy forms of mutant Mbs, approximate peak wavelengths were determined at 4 °C as previously reported (Adachi et al., 1991).

Proton Nuclear Magnetic Resonance (^{1}H-NMR) Spectroscopy. Figure 4 presents hyperfine-shifted ^{1}H-NMR spectra of ferric forms of wild-type and mutant Mbs at room temperature (23 °C). The intense peaks in these spectra are assigned to the heme methyl groups. For wild-type Mb, the hyperfine-shifted four-heme peripheral methyl peaks are observed at 86.5, 80.3, 67.4, and 48.1 ppm far downfield from the HDO resonance (Morishima et al., 1978; La Mar et al., 1980), while the corresponding signals are located at 53.1, 47.0, 33.0, and 26.0 ppm for H93C Mb and at 37.8, 35.3, and 28.7 ppm for H93Y Mb. The temperature dependence of these signals is depicted in Figure 5, and all signals obey Curie's law. The spectrum of ferric H93C Mb is nearly identical with that of *d*-camphor-bound P-450cam (Figure 6A). While ferric H93Y Mb shows less hyperfine-shifted signals than those of bovine liver catalase, similarity of the spectra characteristics is evident (Morishima & Ogawa, 1982). These results indicate that the electronic structures of the heme of the mutants resemble those of the corresponding heme enzymes. For H93Y Mb, two single proton resonances were detected in a far downfield region at 107.4 and 128.1 ppm. These resonances could be assigned to the meta protons of the iron-bound tyrosine, because biphenyl pendant-capped iron(III) porphyrin mimicking catalase gives a downfield proton

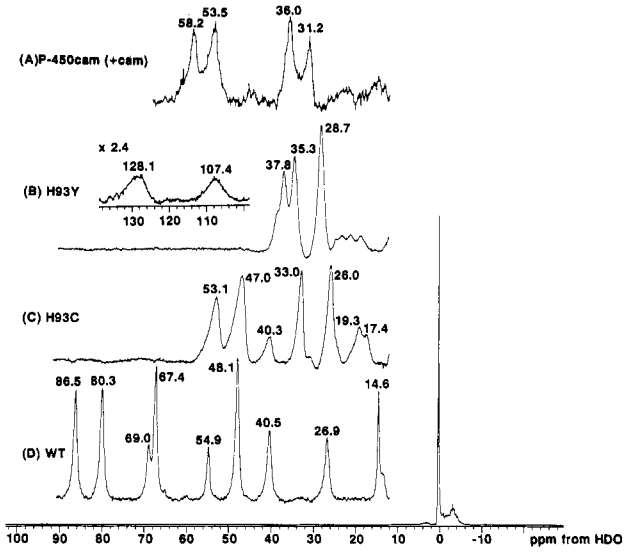

FIGURE 4: ^{1}H-NMR spectra of ferric high-spin forms of (A) P-450cam, (B) H93Y Mb, (C) H93C Mb, and (D) wild-type human Mb in 50 mM sodium phosphate buffer at pD 7.0 and 23 °C. The concentration of the samples is ca. 1 mM.

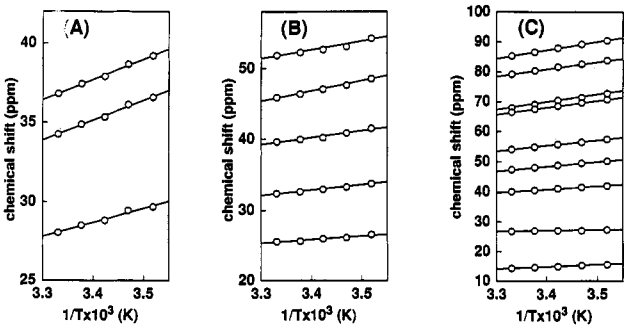

FIGURE 5: Temperature dependence (10–35 °C) of hyperfine-shifted ^{1}H-NMR signals for ferric (A) H93Y Mb, (B) H93C Mb, and (C) wild-type human Mb in 50 mM sodium phosphate buffer at pD 7.0. The chemical shifts are plotted against $1/T \times 10^3$ and are shown by ppm from HDO.

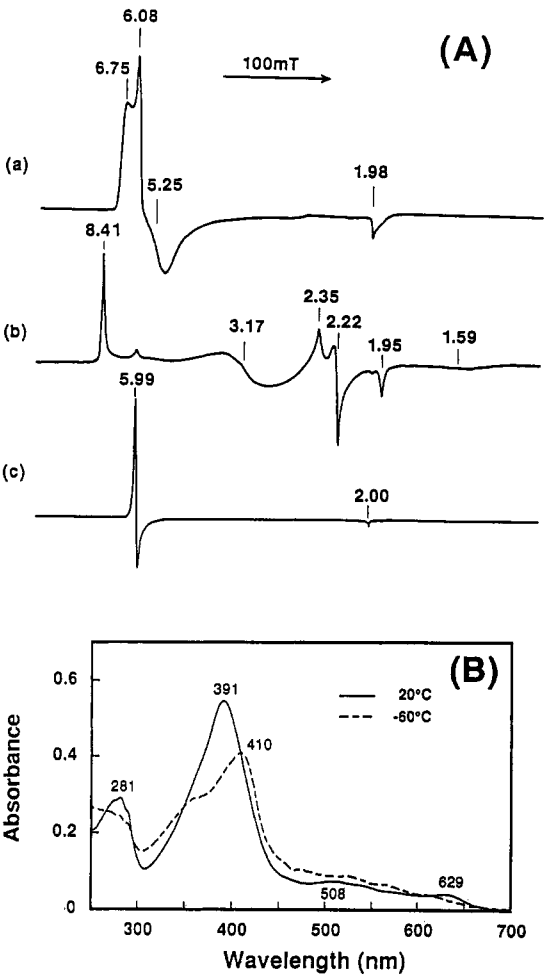

FIGURE 6: (A) EPR spectra of ferric high-spin forms of (a) H93Y Mb, (b) H93C Mb, and (c) wild-type human Mb in 50 mM sodium phosphate buffer at pH 7.0 and 4.2 K. The g values are indicated on the figure. (B) Electronic absorption spectra of ferric H93C Mb at 20 and −60 °C.

resonance at 122.4 ppm for the axially coordinated phenolate meta protons (Garcia et al., 1991). Similar large downfield shifts have been observed for meta protons of phenolate derivatives bound to high-spin ferric iron (Arasasingham et al., 1990; Heistand et al., 1982). Although the axial ligand of the ferric high-spin state of H93C Mb is also expected to give hyperfine-shifted proton signals, they have not been detected yet. An effort was also made to find signals of porphyrin meso protons of the mutants, since the chemical shifts of the signals reflect the coordination number of the heme iron (Budd et al., 1979; La Mar, 1973; Bertini & Luchinat, 1986; Morishima et al., 1985). Unfortunately, such signals are beyond detection probably due to broadening of the signals.

Electron Paramagnetic Resonance (EPR) Spectroscopy. EPR spectra of the ferric forms of the mutants are shown in Figure 6A. H93C Mb gives a mixture of very rhombic high-spin species (g = 8.41, 3.17, 1.59) and low-spin species (g = 2.35, 2.22, 1.95) at 4.2 K similar to the g values reported for ferric P-450 and ferric CPO, indicating that the ligand field of the heme iron for H93C Mb is similar to those for P-450 and CPO (Tsai et al., 1970; Peisach & Blumberg, 1970; Hollenberg et al., 1980). Appearance of the two spin states in these heme proteins is probably caused by a thermal spin equilibrium or ligation of either water or an internal ligand (such as distal histidine) by a freezing effect. As shown in Figure 6B, the peak at 410 nm, characteristic of the low-spin state, is observed upon lowering temperature as a reversible process. These results indicate that the low-spin species appears at low temperature, while the high-spin species is dominant at room temperature. H93Y Mb exhibits multiple g values of 6.75, 6.08, 5.25, and 1.98 which show a ferric high-spin heme with rhombic distortion. These g values are almost the same as those for bovine liver catalase and the His(F8)Tyr mutant of sperm whale Mb (Egeberg et al., 1990; Torii & Ogura, 1968).

Resonance Raman Spectroscopy. Figure 7 presents resonance Raman spectra of the ferric forms of wild-type and mutant Mbs excited at 420 nm. The resultant resonance Raman data for wild-type and mutant Mbs are listed in Table I. According to the high-frequency regions of Figure 7, which are the marker bands of the oxidation (ν_4) and spin and coordination (ν_2, ν_3) states of the heme irons, all the ferric samples are assigned to be in the high-spin state (Felton & Yu, 1978; Spiro, 1983). As exhibited by the ν_3 peak of wild-type Mb at 1483 cm^{-1}, the iron atom is six-coordinate due to a weakly coordinated water molecule as the sixth ligand (Takano, 1977; Spiro & Burke, 1976; Kitagawa et al., 1976; Spiron et al., 1979; Teraoka & Kitagawa, 1980). On the other hand, H93C and H93Y Mbs show significant upshift of the ν_3 and ν_2 marker bands to around 1490 and 1570 cm^{-1}, respectively. These shifts associate with the smaller core size of five-coordinate, high-spin iron (Spiro & Burke, 1976;

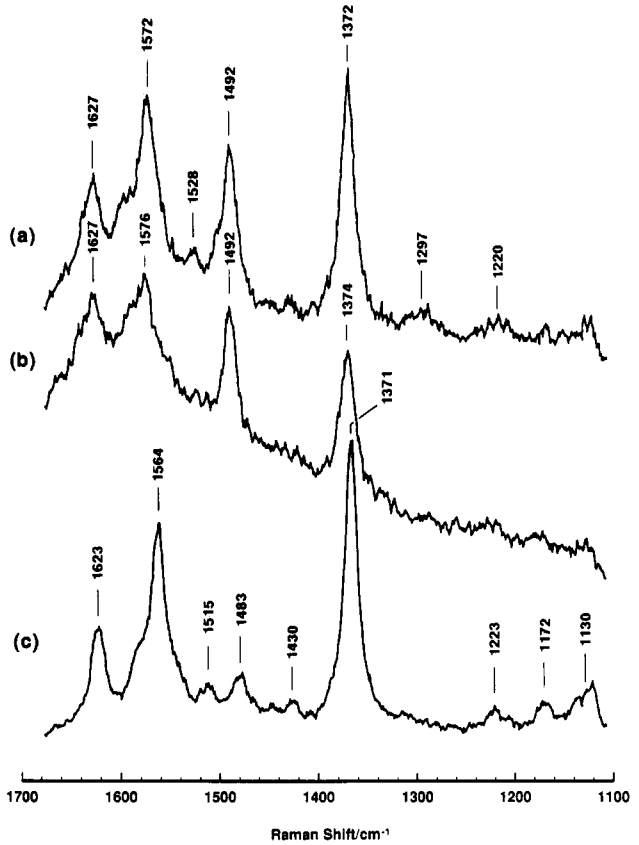

FIGURE 7: Resonance Raman spectra of ferric high-spin forms of (a) H93Y Mb, (b) H93C Mb, and (c) wild-type human Mb in 50 mM sodium phosphate buffer at pH 7.0. The laser excitation wavelength is 420 nm. The power at the sample is 8 mW. The concentration of the samples is 30 μM.

Table I: Raman Frequencies (cm^{-1}) for Mutant and Wild-Type Human Myoglobins by Soret Excitation

mode	H93C Mb	H93Y Mb	wild-type Mb
	Ferric High-Spin/420-nm Excitation		
ν_2	1576	1572	1564
ν_3	1492	1492	1483
ν_4	1374	1372	1371
	Ferrous High-Spin/441.6-nm Excitation		
ν_2	1563	1562	1561
ν_3	1470	1465	1467
ν_4	1357	1354	1355
ν_{Fe-His}	218	219	221
	Ferrous–CO/420-nm Excitation		
ν_2	1576	1586	1586
ν_3	1502	1502	absent
ν_4	1372	1373	1372
ν_{Fe-CO}	502, 526	497, 528	505

Kitagawa et al., 1976; Spiro et al., 1979; Teraoka & Kitagawa, 1980).

In Figures 8 and 9, the laser excitations are moved to 363.8 and 488.0 nm in order to examine the iron–cysteine or iron–tyrosine charge-transfer transition enhanced resonance Raman bands. The coordination of cysteine to the iron in ferric H93C Mb is verified by the enhancement of the cysteine-specific ν_{Fe-S} band by 363.8-nm excitation as shown in Figure 8. The ν_{Fe-S} band for H93C Mb is observed at ca. 350 cm^{-1}. This band corresponds to the ν_{Fe-S} frequencies for P-450cam (351 cm^{-1}) and CPO (347 cm^{-1}) (Champion et al., 1982; Bangcharoenpaurpong et al., 1986). The ν_{Fe-S} band of H93C splits into doublet peak at 343 and 363 cm^{-1}, and such a doublet peak is also encountered in P-450 and CPO at low temperature. Bangcharoenpaurpong et al. (1986, 1987) suggested that the

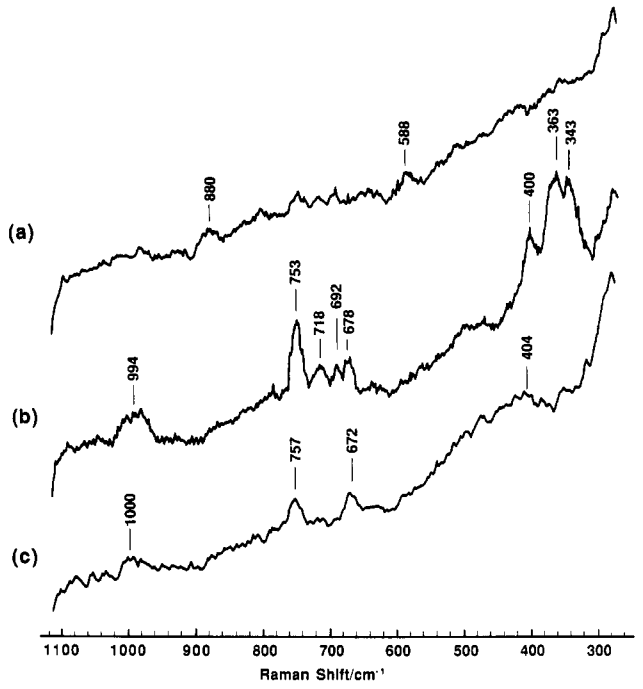

FIGURE 8: Resonance Raman spectra of ferric high-spin forms of (a) H93Y Mb, (b) H93C Mb, and (c) wild-type human Mb in 50 mM sodium phosphate buffer at pH 7.0. The laser excitation wavelength is 363.8 nm. The power at the sample is 20 mW. The concentration of the samples is 50 μM.

transition from high spin state to low spin state caused the splitting of the peak when the excitation wavelength is tuned to longer. Although a low-spin species was detected as a small shoulder of the marker band ν_3 in P-450cam, we cannot find such low-spin species around the ν_3 band for H93C Mb, indicating that the doublet ν_{Fe-S} band of H93C Mb is not caused by the low-spin species.

On the other hand, the presence of the iron–tyrosine linkage in ferric H93Y Mb is demonstrated by the enhanced tyrosine-specific ν_{Fe-O} at 585 cm^{-1} and the internal tyrosine modes $\nu_{C=C}$ and ν_{C-O} at 1504 and 1302 cm^{-1}, respectively (Figure 10) (Nagai et al., 1989, 1983; Chuang et al., 1988; Sharma et al., 1989). These modes are scarcely observable in the Soret excited spectra but show a dramatic increase in relative intensity upon shift of the laser excitation from the Soret band to 488.0 nm (Nagai et al., 1983; Sharma et al., 1989). Table II summarizes the resonance Raman frequencies for heme proteins in which Tyr is ligated to the heme iron. The ν_{Fe-O} and/or internal tyrosine modes ($\nu_{C=C}$ and ν_{C-O}) are observed for all the proteins listed in Table II nearly at the same positions.

Figure 10 displays Soret excited Raman spectra of deoxy Mbs. The frequencies of ν_2 (ca. 1561 cm^{-1}), ν_3 (ca. 1467 cm^{-1}), and ν_4 (ca. 1355 cm^{-1}) are indicative of the five-coordinate high-spin ferrous heme for all samples. In a low-frequency region, the 221-cm^{-1} ν_{Fe-His} mode is enhanced for wild-type Mb (Kitagawa et al., 1979; Choi & Spiro, 1983; Argade et al., 1984) and the observation of the bands at 218 and 219 cm^{-1} for H93C and H93Y Mbs suggests the distal histidine E7 coordination. Figure 11 presents the Raman spectra of the CO-bound samples. The ν_{Fe-CO} vibration is observed at near 500 cm^{-1} for wild-type, H93C, and H93Y Mbs, suggestive of histidine ligation to the heme irons (Tsubaki et al., 1982; Yu & Kerr, 1988). The ν_{Fe-CO} vibration mode was assigned by isotope shift using $^{13}C^{18}O$ (data not shown). Under the conditions employed in our experiments, laser photolysis of the CO complexes of Mbs afforded residual deoxy

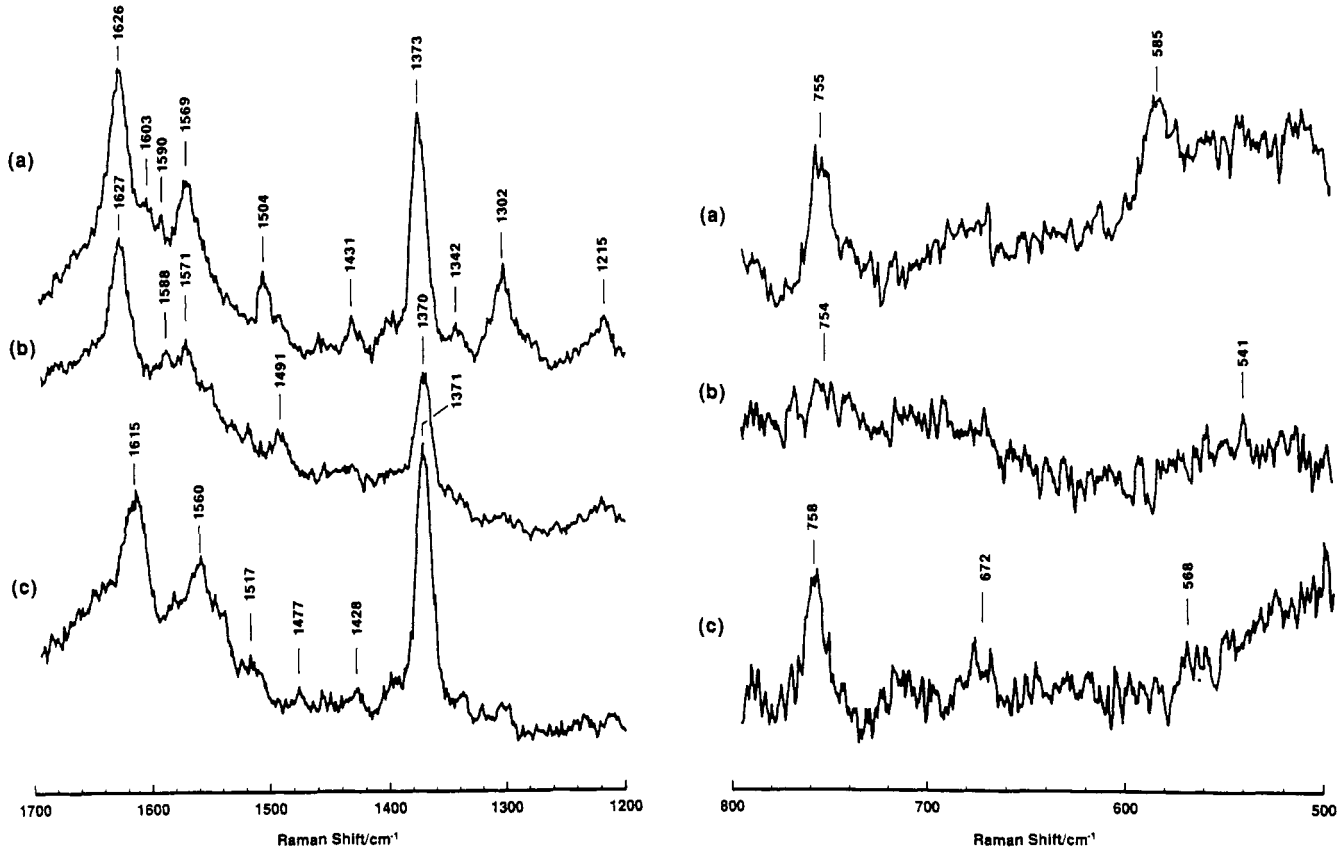

FIGURE 9: Resonance Raman spectra of ferric high-spin forms of (a) H93Y Mb, (b) H93C Mb, and (c) wild-type human Mb in 50 mM sodium phosphate buffer at pH 7.0. The laser excitation wavelength is 488.0 nm. The power at the sample is 80 mW. The concentration of the samples is 200 μM.

species as shown in Figure 11 [denoted by asterisks (*)]. The ν_{Fe-CO} bands of the mutant Mbs show doublets at ca. 500 and 527 cm^{-1}, suggesting the existence of at least two conformers (Tsubaki et al., 1982; Yu & Kerr, 1988; Ramsden & Spiro, 1989).

Reactions of Ferric Wild-Type and Mutant Mbs with Cumene Hydroperoxide. In order to examine the roles of the anionic axial ligand on the O–O bond cleavage, reactions of the ferric forms of wild-type and mutant Mbs with cumene hydroperoxide were examined. Heterolytic O–O bond cleavage of cumene hydroperoxide will afford compound I and cumyl alcohol (eq 3). On the other hand, homolytic cleavage of the O–O bond generates compound II and $PhC(CH_3)_2O^{\bullet}$ (eq 4) with subsequent elimination of methyl radical to give acetophenone (eq 5). Thus, the production of $PhC(CH_3)_2OH$

$$PorFe^{III} + PhC(CH_3)_2OOH \rightarrow Por^{+\bullet}Fe^{IV}{=}O + PhC(CH_3)_2OH \quad (3)$$

$$PorFe^{III} + PhC(CH_3)_2OOH \rightarrow PorFe^{IV}{=}O + PhC(CH_3)_2O^{\bullet} + H^{+} \quad (4)$$

$$PhC(CH_3)_2O^{\bullet} \rightarrow PhC(O)CH_3 + CH_3^{\bullet} \quad (5)$$

and $PhC(O)CH_3$ in the reaction of cumene hydroperoxide with wild-type and mutant Mbs was examined by HPLC, and the time courses of product formation are shown in Figure 12 (see Table III for product analysis). Under the reaction conditions employed, high-valent species such as compounds I and II were not observed because of facile degradation of hemes as visualized by decreased absorbance of the Soret bands (Figure 13). Apparently, wild-type Mb reacts with cumene hydroperoxide by heterolytic and homolytic reaction mechanisms. The proximal Cys mutant Mb enhances the heterolytic O–O bond cleavage, while the proximal Tyr mutant slightly affects the O–O bond scission ratio compared with that of wild-type Mb.

Monooxygenase and Catalase Activities. Epoxidation of styrene, N-demethylation of *N,N*-dimethylaniline, and dismutation of hydrogen peroxide were examined, and the initial reaction rates of these reactions are listed in Table IV. Addition of H_2O_2 to a solution of styrene and wild-type Mb gave an intermediate with shift of the Soret band from 408 to 421 nm, characteristic of the ferryl (Fe^{IV}=O) complex (compound II). This spectral shift was followed by time-dependent irreversible loss of the heme chromophore. On the other hand, the addition of H_2O_2 to H93C and H93Y Mbs caused gradual loss of the Soret band without shift. The styrene metabolites by ferric Mb and H_2O_2 were detected by GLC and identified as styrene oxide, benzaldehyde, and phenylacetaldehyde in comparison with authentic samples. Because of the formation of benzaldehyde and phenylacetaldehyde being small relative to styrene oxide, we determined the reaction rate only for styrene oxide. Initial reaction rates of epoxidation of styrene oxide by H93C and H93Y Mbs were 5.1 and 1.1 times faster than that by wild-type Mb, respectively. Epoxidation of styrene by using hydrogen peroxide and bovine Hb has been reported by Ortiz de Montellano and Catalano (1985), and the reaction rate for human wild-type Mb roughly agrees with the result of bovine Hb. Furthermore, the absolute chirality of styrene oxide formed was examined by using chiral high-pressure liquid chromatography (Figure 14). As listed in Table IV, the ratio of two enantiomers (*R*:*S*) is nearly 1:1 for all proteins. The activity of N-demethylation of *N,N*-dimethylaniline for H93C

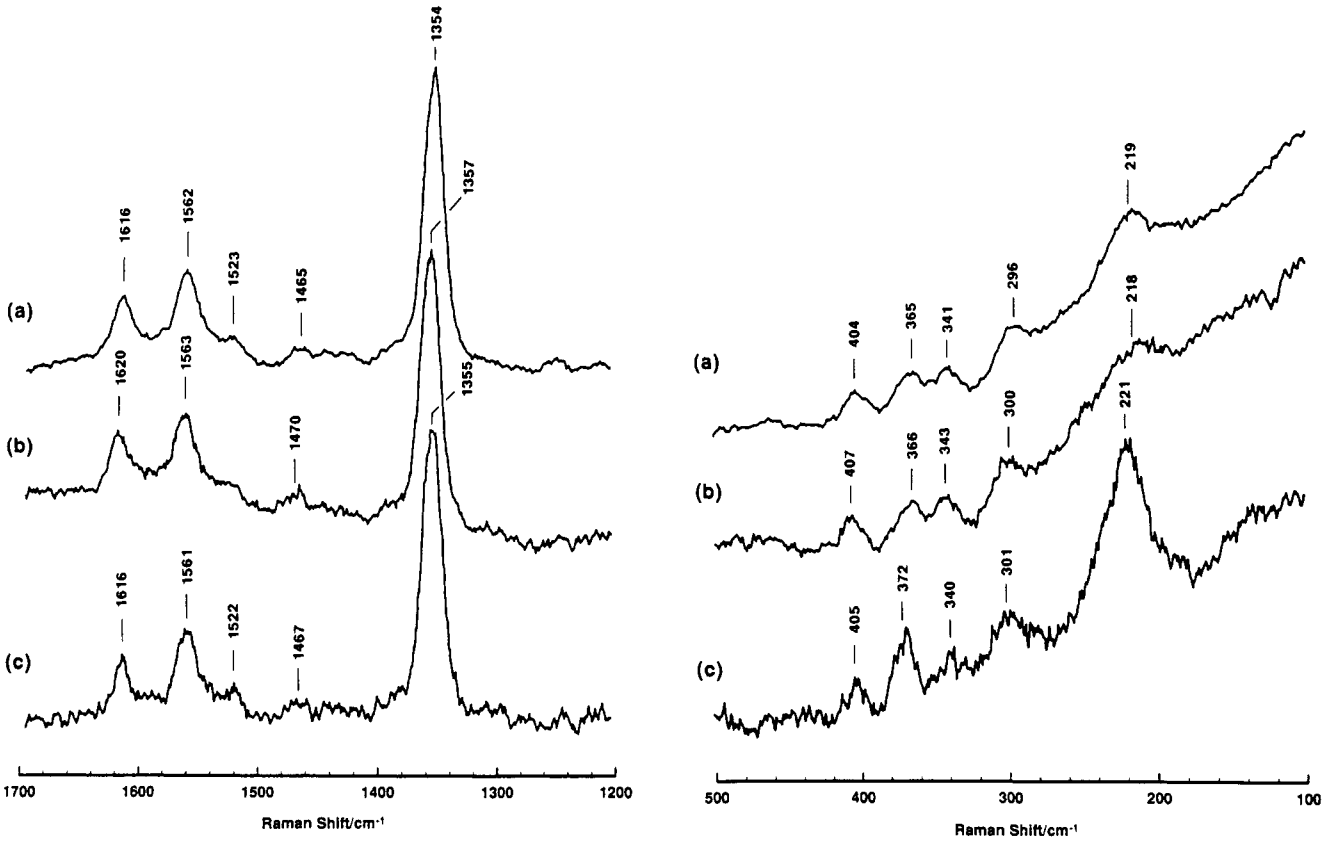

FIGURE 10: Resonance Raman spectra of ferrous high-spin forms of (a) H93Y Mb, (b) H93C Mb, and (c) wild-type human Mb in 50 mM sodium phosphate buffer at pH 7.0. The laser excitation wavelength is 441.6 nm. The power at the sample is 25 mW. The concentration of the samples is 30 μM.

Table II: Raman Frequencies for Ferric High-Spin State of Mutant and Wild-Type Mbs, Catalases, Mutant Human Hbs, and Mutant Sperm Whale Mb at 488.0-nm Excitation

mode	human H93Y Mb	human WT Mb	bovine liver catalase[a,b]	*A. nigar* catalase[b]	*M. luteus* catalase[b]	Hb M Iwate[c]	Hb M Hyde Park[c]	SWMb H93Y[d]
ν_{10}	1626	1615	1625	1625	1626	1628	1628	1630
ν_2	1569	1560	1568	1574	1570	~1570	1567	~1570
ν_3	ND[e]	1477	1484	1489	1489	ND	1489	ND
ν_4	1373	1371	1373	1373	1373	1372	1372	1375
$\nu_{Tyr(C=C)}$	1603	absent	1612	1615	1610	1607	1609	ND
$\nu_{Tyr(C=C)}$	1504	absent	1520	ND	ND	1504	1502	1506
$\nu_{TyrC-O)}$	1302	absent	1244	1245	ND	1308	1300	1303
ν_{Fe-O}	585	absent	ND	ND	ND	588	588	586

[a] Chuang et al., 1988. [b] Sharma et al., 1989. [c] Nagai et al., 1983, 1989. [d] Egeberg et al., 1990. [e] ND, not detected.

Mb is about 2-fold greater, while that for H93Y Mb is about 4-fold smaller, than that for wild-type Mb. The H_2O_2 dismutation activities for H93C and H93Y Mbs are about 3-fold smaller than those for wild-type Mb.

DISCUSSION

Ferric High-Spin State. As shown in Results, the alteration of the proximal histidine of human myoglobin to cysteine or tyrosine caused spectroscopic features of the mutant Mbs being almost identical with those of the corresponding heme enzymes such as P-450, CPO, and catalase (Dawson & Sono, 1987; Dolphin, 1978). Thus, it is clearly shown here that the axial ligand of a heme iron is responsible for the spectroscopic features of heme proteins, which has been suggested by various studies of heme proteins and model heme complexes (Dolphin, 1978).

The EPR spectrum of H93C Mb is unusual among ferric high-spin heme proteins with respect to the rhombic splitting caused by the thiolate ligation. While histidine-bound ferric high-spin heme systems exhibit g values at 6 and 2, ferric high-spin P-450 and CPO give g values at 8.0, 4.0, and 1.8 and at 7.6, 4.3, and 1.8, respectively (Tsai et al., 1970; Peisach & Blumberg, 1970; Hollenberg et al., 1980). Studies of model heme complexes also showed that the rhombic splitting observed in ferric high-spin P-450 could be reproduced with five-coordinate ferric porphyrin–thiolate complexes (Koch et al., 1975; Collman et al., 1975; Ogoshi et al., 1975). As shown in Figure 6A, g values for ferric high-spin H93C Mb are observed at 8.41, 3.17, and 1.59, in agreement with those for the corresponding enzymes and model complexes. Palmer (1979) showed percent rhombicity of several native heme proteins in their ferric high-spin states based on g values in the $g = 6$ region. H93C and H93Y Mbs display high rhombicities (% rhombicity: H93C, 32.8%; H93Y, 8.7%) nearly identical with those reported for P-450cam (26.0%) and bovine liver catalase (type I, 7.5%; type II, 11.7%), respectively. As shown in Figure 6A, ferric H93Y Mb exhibits a typical ferric high-spin spectrum with rhombic distortion resembling ferric bovine liver catalase (Torii & Ogura, 1968; Peisach et al., 1971; Rein et al., 1968; William-Smith & Patel,

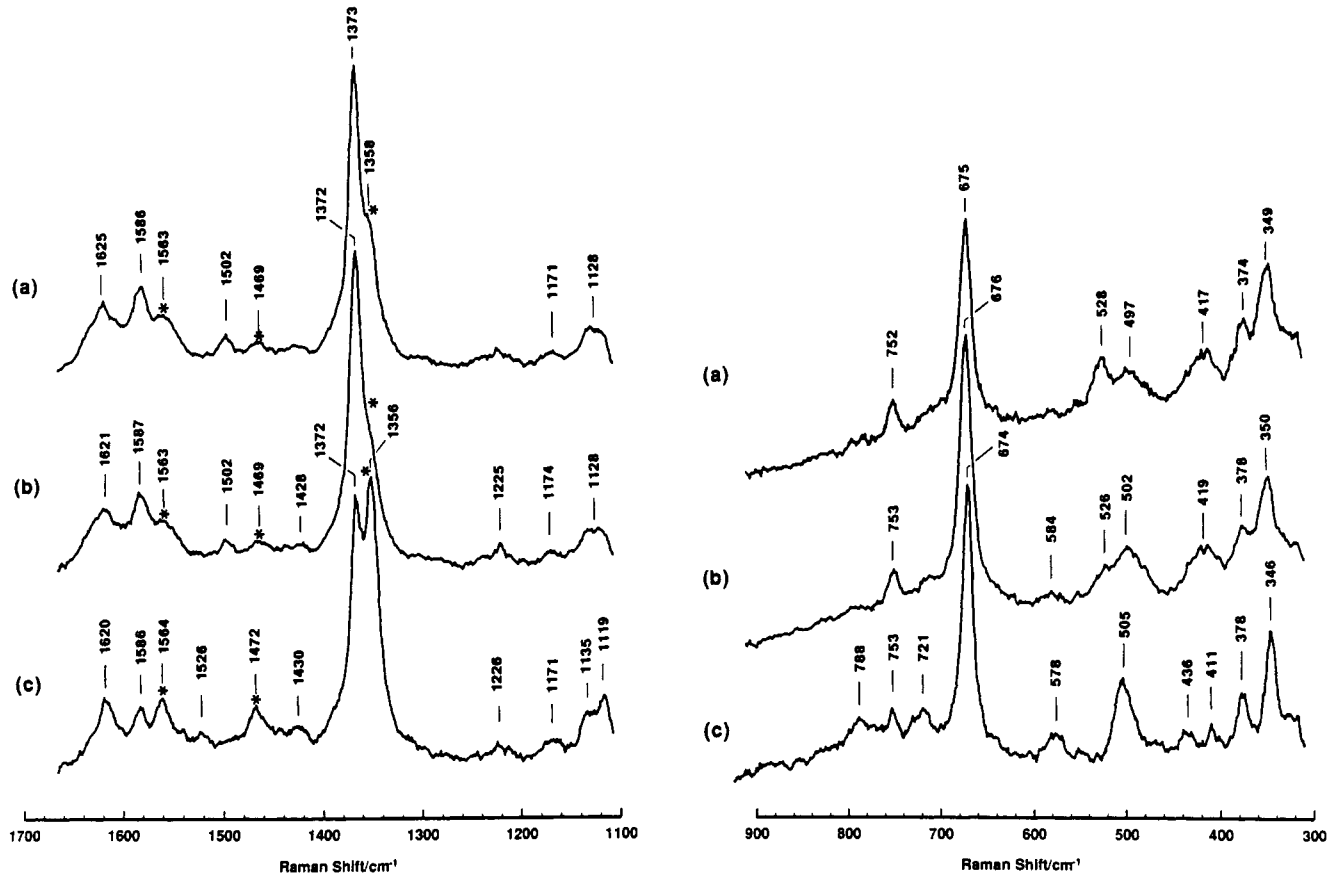

FIGURE 11: Resonance Raman spectra of carbonmonoxy forms of (a) H93Y Mb, (b) H93C Mb, and (c) wild-type human Mb in 50 mM sodium phosphate buffer at pH 7.0. The laser excitation wavelength is 420 nm. The power at the sample is 8 mW. The concentration of the samples is 30 μM. Raman bands responsible for deoxy species due to laser photolysis of CO are denoted by asterisks (*).

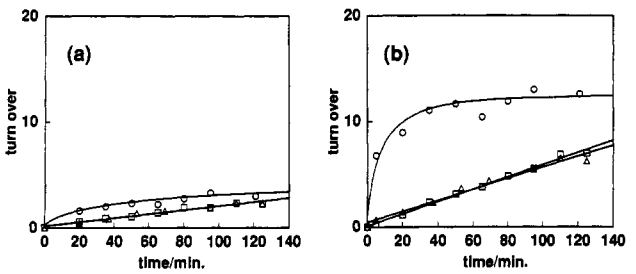

FIGURE 12: Time course of (a) acetophenone and (b) cumyl alcohol formation in the reaction of 10 μM Mbs (□, wild-type Mb; ○, H93C Mb; △, H93Y Mb) and 240 μM cumene hydroperoxide. Experiments were performed in 2 mL of 50 mM sodium phosphate buffer, pH 7.0, 20 °C.

Table III: Product Analysis of Reactions of Ferric Heme Proteins with Cumene Hydroperoxide

	$PhC(CH_3)_2OH^a$	$Ph(CH_3)C{=}O^b$	hetero/homo[c]
WT	0.13	0.04	3.2
H93C	2.72	0.38	7.2
H93Y	0.15	0.05	2.8

[a] μM cumyl alcohol/(2 min·μM heme). [b] μM acetophenone/(2 min·μM heme). [c] *a*/*b*.

1975; William-Smith & Morrison, 1975). Analogous Hb mutants show similar but slightly different EPR spectra (Hb M Iwate, g = 6.2 and 5.8; Hb M Hyde Park, g = 6.31, 5.68, and 2.0) (Hayashi et al., 1969).

It is worthwhile to discuss the hyperfine-shifted proton NMR spectra of H93Y Mb in relation to those of natural mutant Hb Iwate [His(αF8) → Tyr] and of model iron(III) porphyrins with axial phenoxide. It has been reported that the nonexchangeable single-proton peaks were observed at 78, 91, and 122 ppm for Hb M Iwate, and these are assigned to the coordinated tyrosinate meta hydrogens and/or two nonequivalent protons of the β-CH_2 of the tyrosine side chain, on the basis of the hyperfine shifts for the five-coordinate high spin

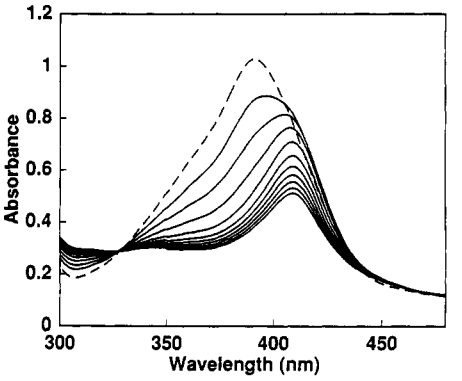

FIGURE 13: Time-dependent spectral changes of the H93C Mb (1-min interval) in the reaction of H93C Mb and cumene hydroperoxide. The dashed line shows the spectrum in the absence of cumene hydroperoxide. Conditions were the same as in Figure 12.

Table IV: Initial Rates of Catalytic Reactions and Enantiomer Ratio of Styrene Oxide

	epoxidation of styrene[a]	enantiomer ratio (*R*:*S*)[b]	N-demethylation of *N*,*N*-dimethylaniline[c]	dismutation of H_2O_2[d]
WT	1.8×10^{-2}	48:52	107	1.1
H93C	9.2×10^{-2}	51:49	213	0.32
H93Y	1.9×10^{-2}	~50:50	24	0.46

[a] μM styrene oxide/(2 min·μM heme). [b] Determined by chirality sensitive HPLC. [c] μM HCHO/(min·μM heme). [d] μM H_2O_2/μM heme.

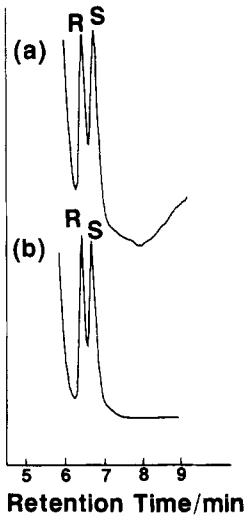

FIGURE 14: High-pressure liquid chromatogram of diastereomeric styrene oxide mixture formed in the epoxidation of styrene by ferric (a) wild-type and (b) H93C Mbs.

iron(III) porphyrins with axial phenoxide ligands (La Mar et al., 1980; Arasasingham et al., 1990). While we have tentatively assigned resonances at 107.4 and 128.1 ppm for H93Y Mb to the metal hydrogens on the basis of recent chemical model studies (Garcia et al., 1991), the β-CH_2 of the tyrosine side chain is an alternative candidate.

Direct evidence for the thiolate ligand bound to the ferric heme iron of H93C Mb in the high-spin state is derived from the resonance Raman spectroscopy. As depicted in Figure 8, the band at ca. 350 cm^{-1} observed for H93C Mb with 363.8-nm excitation is not observed for wild-type and H93Y Mbs, indicative of cysteine ligation in H93C Mb. Further, this value is consistent with the ν_{Fe-S} frequencies observed for ferric P-450cam and CPO. Champion et al. (1982) and Bangcharoenpaurpong et al. (1986) studied ^{34}S-labeled derivatives of both ferric high-spin P-450cam and CPO with resonance Raman spectroscopy using laser excitation at 363.8 nm. The Fe–S vibration modes at 351 and 347 cm^{-1} for P-450cam and CPO, respectively, were selectively shifted for the ^{34}S-labeled enzymes. Thus, these observations provided the direct evidence for cysteine ligations in ferric H93C Mb, P-450cam, and CPO. The tyrosine ligation in H93Y Mb is also spectroscopically confirmed by the selected resonance-enhanced tyrosine vibrational modes. As shown in Figure 9, the resonance Raman spectrum of ferric H93Y Mb exhibits the tyrosine-specific mode (ν_{Fe-O} and internal tyrosine modes ($\nu_{C=C}$ and ν_{C-O}) at 585, 1504, and 1302 cm^{-1}. In the case of catalases, while the ν_{Fe-O} mode was obscured by the neighboring vibrational porphyrin modes, the tyrosine ring mode ($\nu_{C=C}$) at 1612 cm^{-1} was enhanced with 488.0-nm excitation (Chuang et al., 1988; Sharma et al., 1989). Other tyrosine modes, $\nu_{C=C}$ and ν_{C-O}, have been assigned to 1520 and 1245 cm^{-1}, respectively, for bovine liver catalase (Chuang et al., 1988). In addition, resonance Raman spectra of ferric forms of Hb M Iwate, Hb M Hyde Park, and proximal F8 tyrosine mutant of sperm whale Mb also exhibit similar types of spectra as listed in Table II (Egeberg et al., 1990; Nagai et al., 1983, 1989).

The most characteristic modes of the coordination and spin state of heme irons are ν_3 and ν_2 (Spiro & Burke, 1976; Kitagawa et al., 1976; Spiro et al., 1979; Teraoka & Kitagawa, 1980). For five-coordinate high-spin hemes, the ν_3 and ν_2 bands should be located in the range of 1487–1494 and 1565–1576 cm^{-1}, respectively. These modes for ferric P-450, CPO, and catalase are observed in this range. As listed in Table I, the peak frequencies of these modes for ferric H93C and H93Y Mbs are also in this region, indicating that these proteins are in the same ligation state with ferric high-spin, five-coordinate structure.

Redox potentials of the present human Mb mutants (H93C Mb, –230 mV; H93Y Mb, –190 mV) have been reported previously (Adachi et al., 1991). Important structural factors that control the reduction potential of redox proteins are (1) the nature of ligand(s) at the redox center and (2) electrostatic interactions of the redox center with charged groups both on the surface and in the interior of the protein. Concerning the electrostatic interaction effects, Varadarajan et al. (1989b) have recently examined the effects of ionizable amino acids buried in the protein on the redox potentials of recombinant human Mb. They replaced Val68(E11) of human Mb by potentially charged residues (Glu, Asp) and uncharged but polar Asn. The redox potentials (ferric/ferrous couple) of these mutants were –136.8, –132.2, and –23.8 mV for Glu, Asp, and Asn mutants at 25 °C, respectively, considerably lower than that of wild-type Mb (+50 mV). These results can be interpreted in terms of stabilization of positively charged ferric heme iron by the negative charge at residue 68. The anionic nature of the ligand coordinated to the heme iron has been also assumed to lower redox potential. Heme enzymes such as P-450cam (high spin, –170 mV; low spin, –270 mV), horseradish peroxidase (–250 mV), and catalase (<–500 mV) have their redox potentials much lower than that of human Mb (+50 mV) due to push effect of the anionic axial ligands (Gunsalus et al., 1974; Yamada et al., 1975; Williams, 1974). It is thus shown here that very low redox potentials of H93C and H93Y Mbs compared with that of wild-type Mb (+50 mV) are caused by the anionic thiolate or phenolate ligation to the heme iron.

Ferrous High-Spin State. A different ligation state of ferrous high-spin H93C Mb from ferrous high-spin P-450 and CPO is suggested by the oxidation marker band (ν_4) at 1357 cm^{-1} (Champion et al., 1976, 1978; Ozaki et al., 1976, 1978; Shimizu et al., 1981; Remba et al., 1979; Chottard et al., 1984; Choi et al., 1982). This band is located in the range of 1341–1348 cm^{-1} for P-450, CPO, and thiolate-ligated models, while the corresponding bands for ferrous Mb, Hb, and horseradish peroxidase appear in the range of 1355–1360 cm^{-1}. The downshift of the ν_4 band, which is a C–N stretching mode, for P-450 and CPO has been attributed to the presence of a strongly electron-donating π-base such as a thiolate that pushes electrons to the porphyrin π^*-antibonding orbitals to weaken the porphyrin bond strength. The present finding and the Fe–His stretching band at 218 cm^{-1} for H93C Mb could suggest that distal His64(E7) is ligated to the ferrous iron. The broad Fe–His stretching band shown in Figure 10 would be attributed to inhomogeneous broadening caused by possible distribution of distal His–Fe binding mode.

Due to difficulty of preparing the ferrous state of catalase, we compare ferrous H93Y Mb with the corresponding mutant of sperm whale Mb (Egeberg et al., 1990). The ferrous H93Y Mb being in five-coordinate high-spin state is confirmed by resonance Raman spectroscopy (Figure 10). Although the ν_{Fe-His} band was not observed for the ferrous His(F8)Tyr mutant of sperm whale Mb (Egeberg et al., 1990), we found this band at 219 cm^{-1} for ferrous H93Y Mb. The difference could be caused by subtle structural differences between sperm whale and human Mb. Thus, the weak band at 219 cm^{-1} assigned to ν_{Fe-His} for the human Mb mutant suggests that distal His E7 is coordinated to the ferrous heme iron.

Carbon Monoxide-Bound Derivatives. Since the appearance of the ν_{Fe-His} mode in the resonance Raman spectra of ferrous high-spin H93C and H93Y Mbs suggests the ligation of imidazole of distal His to the ferrous heme iron, it is likely that CO is bound to the ferrous heme iron in the proximal pocket rather than the distal pocket. The CO adducts of H93C and H93Y Mbs exhibit ν_{Fe-CO} vibrations at ca. 500 cm^{-1}, typical of histidine-coordinated heme proteins with the relatively upright binding geometry of CO, and at ca. 530 cm^{-1}, suggestive of five-coordinate monocarbonyl adducts (Tsubaki et al., 1982; Yu & Kerr, 1988; Ramsden & Spiro, 1989). Since the CO and NO complexes of Hb M Iwate (Peisach & Gersonde, 1977; Nagai et al., 1979) were shown to have the heme environmental structure with distal His ligated to the ferrous heme iron, EPR spectra of NO adducts of H93C and H93Y Mbs were measured at 77 K (data not shown). A triplet signal arising from ^{14}NO was not further split by the superhyperfine interaction with the iron-bound His, just like cyanogen bromide-modified MbNO and α-chain of Hb A bound with inositol hexaphosphate, where histidine ligand comes off upon NO coordination (Morishima et al., 1989; Maxwell & Caughey, 1976; Szabo & Perutz, 1976). Thus, NO adducts of H93C and H93Y Mbs are likely in a five-coordinate structure.

Reactions of Ferric Forms of Wild-Type and Mutant Mbs with Peroxides. Addition of several equivalents of H_2O_2 to a solution of ferric wild-type Mb at room temperature is known to afford an Fe^{IV}=O complex closely related to compound II of HRP (Penner-Hahn et al., 1983; Morishima & Ogawa, 1978a–c; La Mar et al., 1983). Since H_2O_2 has two oxidizing equivalents, George and Irvine (1952, 1956) demonstrated that the remaining oxidation equivalent of the H_2O_2-oxidized Mb is retained by the protein and proposed (1) that homolysis of H_2O_2 by Mb yields the hydroxyl radical and an Fe^{IV}=O complex or (2) that heterolysis yields a $Por^{+\bullet}Fe^{IV}$=O complex, which is reduced rapidly to the Fe^{IV}=O species by the protein. On the other hand, reaction of H_2O_2 with H93C or H93Y Mb resulted in an irreversible loss of the Soret band, even at −40 °C in the presence of 60% glycerol (data not shown). Therefore, a different reaction could proceed in the reaction of the mutants with H_2O_2, and this prompted us to examine the reaction product of cumene hydroperoxide.

Bruice and co-workers have examined reactions of model heme complexes with various alkyl and acyl hydroperoxides (Balasubramanian et al., 1989; Murata et al., 1990). They reported that reaction of water-soluble iron(III) porphyrin with cumene hydroperoxide at pH 7.25 gave acetophenone as the sole product (77%) according to the homolytic O–O bond cleavage (Balasubramanian et al., 1989). In the case of wild-type Mb, the O–O bond of cumene hydroperoxide is cleaved both by a heterolytic pathway and by a homolytic mechanism (Table III). Thus, the formation of compound II in the reaction of ferric wild-type Mb with H_2O_2 is the result of two mechanisms [(1) and (2)] proposed by George and Irvine (1952, 1956). In contrast, H93C Mb and cumene hydroperoxide predominantly yield cumyl alcohol (Figure 12). In this reaction, addition of cumene hydroperoxide caused the Soret band shift from 391 to 410 nm in a few minutes followed by the loss of the Soret band at 410 nm (Figure 13). Inspection of Figures 12 and 13 indicates that the formation of cumyl alcohol was suppressed with concomitant shift of the Soret band from 391 to 410 nm. These observations imply that the rapid formation of cumyl alcohol at the early stage of the reaction is attributed to the reaction of cumene hydroperoxide with H93C Mb, but not with a denatured product. These results favor the active intermediate in the catalytic cycle of P-450 being compound I or its oxyradical resonant structure. It is interesting to note that the distal pocket of P-450cam consists of hydrophobic amino acid residues (Poulos et al., 1985), and few residues exist to potentially assist the heterolytic O–O bond cleavage by a "pull" mechanism which is proposed in the case of CCP (Poulos & Kraut, 1980). Thus, an anionic thiolate ligand is expected to play a key role in the heterolytic O–O bond cleavage by P-450. Further, increase of catalytic reactivities such as epoxidation of styrene and N-demethylation of *N,N*-dimethylaniline for H93C Mb (Table IV) could be due to the enhanced heterolytic O–O bond cleavage.

The reaction of P-450 with peroxyphenylacetic acid ($PhCH_2CO_3H$) was examined by White and co-workers (White et al., 1980; McCarthy & White, 1983). Contrary to our results, they indicated the homolytic mechanism of O–O bond cleavage is dominant on the basis of the production of benzyl alcohol which is generated from benzyl radical, a decarboxylated product of phenylacetoxy radical ($PhCH_2CO_2^{\bullet}$). However, they have not determined the amount of phenylacetic acid formed by heterolytic O–O bond cleavage. In addition, the spectral changes according to the reaction with peracid must be examined to make sure of the possible participation of denatured enzyme. Further, slow decomposition of peroxyphenylacetic acid to form phenylacetic acid was observed in 0.1 M sodium phosphate buffer (pH 7.0). The nonenzymic decomposition of phenylperacetic acid prevented us from determining the exact amount of phenylacetic acid formed by the heterolysis of O–O bond.[1] Thus, it is important to examine the time-dependent spectral changes and product distribution by the reaction of P-450 with cumene hydroperoxide, which is in progress in our laboratory. In the case of H93Y Mb, neither homolysis nor heterolysis of the O–O bond cleavage reaction is enhanced by the mutation in comparison with the wild-type Mb. This suggests that amino acids in the close vicinity of the iron-bound peroxide are responsible for the selective formation of compound I of catalase. In fact, bovine liver catalase has His74 and Asn147 residues in the distal pocket which locate at appropriate positions where they can participate in the O–O bond cleavage reaction (Murthy et al., 1981).

Mechanism of the Epoxidation Reaction. While heterolytic O–O bond cleavage of peroxide is enhanced by the His93(F8) → Cys mutation, monooxygenase and catalase activities of the mutants are increased 5-fold at most (Table IV). This could be due to facile degradation of compound I and inaccessibility of the substrate to the active site. In order to examine whether the epoxidation reaction of styrene by the mutants and H_2O_2 proceeds in the heme pocket or not, we have examined the chirality of epoxide by use of chiral HPLC. As shown in Figure 14 and Table IV, the enantiomer ratio (*R*:*S*) is almost 1:1 in wild-type- and mutant Mb-catalyzed reactions, suggesting that the reaction does not take place in the heme pocket for wild-type and mutant Mbs. The mechanism of epoxidation reaction of styrene by Hb was extensively examined by Ortiz de Montellano and Catalano (1985). They showed that this type of oxidation exhibits the following features: (1) the epoxidation proceeds with partial scrambling of the olefin stereochemistry, and (2) the product is almost racemic. The oxidations of styrene by sperm whale and horse Mbs gave similar results. On the basis of these results, Ortiz de Montellano and Catalano (1985) proposed

[1] Most of the peroxyphenylacetic acid (80%) slowly decomposes to form phenylacetic acid in 12 h in 50 mM sodium phosphate buffer (pH 7.0) at 20 °C.

that the oxidative generation of a surface Tyr radical provides the activation of molecular oxygen. Thus, epoxidation reactions by mutant Mbs seems to proceed by the same reaction mechanism as well as wild-type Mb.

In summary, site-directed mutagenesis of histidine-93(F8) in human myoglobin (Mb) to cysteine and tyrosine resulted in altered axial ligations analogous to P-450, CPO, and catalase. Cysteine or tyrosine coordination to the ferric heme iron is confirmed by various spectroscopic methods, and these mutants are revealed to be in the high-spin, five-coordinate state. Redox potentials of ferric/ferrous couple for these mutants (ca. −200 mV) are significantly lower than that for wild-type Mb (+50 mV) due to ligation of the anionic ligand. The ferrous states of H93C and H93Y Mbs are high-spin and five-coordinate, and ligation of distal histidine to the ferrous heme iron is suggested by electronic absorption and resonance Raman spectroscopy. Furthermore, the role of anionic axial ligands on the O–O bond cleavage reaction is examined by utilizing reactions with peroxides. The thiolate ligand dominantly enhanced heterolytic O–O bond cleavage. On the other hand, the phenolate ligand enhanced neither the heterolytic nor the homolytic mechanism of O–O bond cleavage in comparison with wild-type Mb.

ACKNOWLEDGMENT

We are grateful to Dr. R. Varadarajan and Prof. S. G. Boxer (Stanford University) for the gift of expression vector of human myoglobin gene. We are also indebted to Dr. H. Hori (Osaka University) for EPR measurement.

REFERENCES

Adachi, S., Nagano, S., Watanabe, Y., Ishimori, K., & Morishima, I. (1991) *Biochem. Biophys. Res. Commun. 180*, 138–144.

Antonini, E., & Brunori, M. (1971) *Hemoglobin and Myoglobin in Their Reactions with Ligands*, North-Holland, Amsterdam, The Netherlands.

Arasasingham, R. D., Balch, A. L., Cornman, C. R., de Ropp, J. S., Eguchi, K., & La Mar, G. N. (1990) *Inorg. Chem. 29*, 1847–1850.

Argade, P. V., Sassaroli, M., Rousseau, D. L., Inubushi, T., Ikeda-Saito, M., & Lapidot, A. (1984) *J. Am. Chem. Soc. 106*, 6593–6596.

Balasubramanian, P. N., Lee, R. W., & Brucie, T. C. (1989) *J. Am. Chem. Soc. 111*, 8714–8721.

Bangcharoenpaurpong, O., Champion, P. M., Hall, K. S., & Hager, L. P. (1986) *Biochemistry 25*, 2374–2378.

Bangcharoenpaurpong, O., Champion, P. M., Martins, S. A., & Sligar, S. G. (1987) *J. Chem. Phys. 87*, 4273–4284.

Bertini, I., & Luchinat, C. (1986) in *NMR of Paramagnetic Molecules in Biological Systems*, pp 165–229, Benjamin-Cummings, Menlo Park, CA.

Browett, W. R., Gasyna, Z., & Stillman, M. J. (1983) *Biochem. Biophys. Res. Commun. 112*, 515–520.

Budd, D. L., La Mar, G. N., Langry, K. C., Smith, K. M., & Nayyir-Mazhir, R. (1979) *J. Am. Chem. Soc. 101*, 6091–6096.

Champion, P. M., Remba, R. D., Chiang, R., Fitcher, D. B., & Hager, L. P. (1976) *Biochim. Biophys. Acta 446*, 486–492.

Champion, P. M., Gunsalus, I. C., & Wagner, G. C. (1978) *J. Am. Chem. Soc. 100*, 3743–3751.

Champion, P. M., Stallard, B. R., Wagner, G. C., & Gunsalus, I. C. (1982) *J. Am. Chem. Soc. 104*, 5469–5472.

Chance, B. (1943) *J. Biol. Chem. 151*, 553–577.

Chance, B. (1949) *Science 109*, 204–208.

Chance, B., Powers, L., Ching, Y., Poulos, T., Schonbaum, G. R., Yamazaki, I., & Paul, K. G. (1984) *Arch. Biochem. Biophys. 235*, 596–611.

Choi, S., & Spiro, T. G. (1983) *J. Am. Chem. Soc. 105*, 3683–3692.

Choi, S., Spiro, T. G., Langry, K. C., Smith, K. M., Budd, D. L., & La Mar, G. N. (1982) *J. Am. Chem. Soc. 104*, 4345–4351.

Chottard, G., Schappacher, M., Ricard, L., & Weiss, R. (1984) *Inorg. Chem. 23*, 4557–4561.

Chuang, W.-J., Johnson, S., & Van Wart, H. E. (1988) *J. Inorg. Biochem. 34*, 201–219.

Collman, J. P., Sorrell, T. N., & Hoffman, B. M. (1975) *J. Am. Chem. Soc. 97*, 913–914.

Dawson, J. H. (1988) *Science 240*, 433–439.

Dawson, J. H., & Sono, M. (1987) *Chem. Rev. 87*, 1255–1276.

Dawson, J. H., Holm, R. H., Trudell, J. R., Barth, G., Linder, R. E., Bunnenberg, E., Djerassi, C., & Tang, S. C. (1976) *J. Am. Chem. Soc. 98*, 3707–3709.

Dolphin, D. (1978) *The Porphyrins*, Academic Press, New York.

Dolphin, D., Forman, A., Borg, D. C., Fajer, J., & Felton, R. H. (1971) *Proc. Natl. Acad. Sci. U.S.A. 68*, 614–618.

Dunford, H. B. (1982) *Adv. Inorg. Biochem. 4*, 41–68.

Dunford, H. B., & Stillman, J. S. (1976) *Coord. Chem. Rev. 19*, 187–251.

Egeberg, K. D., Springer, B. A., Martinis, S. A., Sligar, S. G., Morikis, D., & Champion, P. M. (1990) *Biochemistry 29*, 9783–9791.

Felton, R. H., & Yu, N.-T. (1978) in *The Porphyrins* (Dolphin, D., Ed.) Vol. 3, pp 346–393, Academic Press, New York.

Garcia, B., Lee, C.-H., Blaskó, A., & Bruice, T. C. (1991) *J. Am. Chem. Soc. 113*, 8118–8126.

George, P. (1953) *J. Biol. Chem. 201*, 413–426.

George, P., & Irvine, D. H. (1952) *Biochem. J. 52*, 511–517.

George, P., & Irvine, D. H. (1956) *J. Colloid Sci. 11*, 327–339.

Groves, J. T., & Watanabe, Y. (1988) *J. Am. Chem. Soc. 110*, 8443–8452.

Groves, J. T., Haushalter, R. C., Nakamura, M., Nemo, T. E., & Evans, B. J. (1981) *J. Am. Chem. Soc. 103*, 2884–2886.

Gunsalus, I. C., Meeks, J. R., Lipscomb, J. D., Debrunner, P., & Münk, E. (1974) in *Molecular Mechanisms of Oxygen Activation*, pp 559, Academic Press, New York.

Harrison, J. R., Araiso, T., Palcic, M. M., & Dunford, H. B. (1980) *Biochem. Biophys. Res. Commun. 94*, 34–40.

Hayashi, A., Suzuki, T., Imai, K., Morimoto, H., & Watari, H. (1969) *Biochim. Biophys. Acta 194*, 6–15.

Heistand, R. H., II, Lauffer, R. B., Fikrig, E., & Que, L., Jr. (1982) *J. Am. Chem. Soc. 104*, 2789–2796.

Hewson, W. D., & Hager, L. P. (1979) in *The Porphyrins* (Dolphin, D., Ed.) Vol. 7, Part B, pp 295–332, Academic Press, New York.

Hollenberg, P. F., Hager, L. P., Blumberg, W. E., & Peisach, J. (1980) *J. Biol. Chem. 255*, 4801–4807.

Kitagawa, T., Kyogoku, Y., Iizuka, T., & Ikeda-Saito, M. (1976) *J. Am. Chem. Soc. 98*, 5169–5173.

Kitagawa, T., Nagai, K., & Tsubaki, M. (1979) *FEBS Lett. 104*, 376–378.

Koch, S., Tang, S. C., Holm, R. H., Frankel, R. B., & Ibers, J. A. (1975) *J. Am. Chem. Soc. 97*, 916–918.

La Mar, G. N. (1973) in *NMR of Paramagnetic Molecules, Principles and Applications* (La Mar, G. N., Horrocks, W. DeW., Jr., Holm, R. H., Eds.) pp 86–126, Academic Press, New York.

La Mar, G. N., Budd, D. L., Smith, K. M., & Langry, K. C. (1980) *J. Am. Chem. Soc. 102*, 1822–1827.

La Mar, G. N., de Ropp, J. S., Smith, K. M., & Langry, K. C. (1981) *J. Biol. Chem. 256*, 237–243.

La Mar, G. N., de Ropp, J. S., Latos-Grazynski, L., Balch, A. L., Johnson, R. B., Smith, K. M., Parish, D. W., & Cheng, R.-J. (1983) *J. Am. Chem. Soc. 105*, 782–787.

Maguire, R. J., Dunford, H. B., & Morrison, M. (1971) *Can. J. Biochem. 49*, 1165–1171.

Maxwell, J. C., & Caughey, W. S. (1976) *Biochemistry 15*, 388–396.

McCarthy, M.-B., & White, R. E. (1983) *J. Biol. Chem. 258*, 9153–9158.
Morishima, I., & Ogawa, S. (1978a) *Biochem. Biophys. Res. Commun. 83*, 946–953.
Morishima, I., & Ogawa, S. (1978b) *Biochemistry 17*, 4384–4388.
Morishima, I., & Ogawa, S. (1978c) *J. Am. Chem. Soc. 100*, 7125–7127.
Morishima, I., & Ogawa, S. (1982) in *Oxidases and Related Redox Systems* (King, T. E., et al., Eds.) p 599, Pergamon Press, Oxford and New York.
Morishima, I., Ogawa, S., Inubushi, T., & Iizuka, T. (1978) *Adv. Biophys. 11*, 217–245.
Morishima, I., Shiro, Y., & Takamuki, Y. (1983) *J. Am. Chem. Soc. 105*, 6168–6170.
Morishima, I., Takamuki, Y., & Shiro, Y. (1984) *J. Am. Chem. Soc. 106*, 7666–7672.
Morishima, I., Shiro, Y., & Wakino, T. (1985) *J. Am. Chem. Soc. 107*, 1063–1065.
Morishima, I., Shiro, Y., & Nakajima, K. (1986) *Biochemistry 25*, 3576–3584.
Morishima, I., Shiro, Y., Adachi, S., Yano, Y., & Orii, Y. (1989) *Biochemistry 28*, 7582–7586.
Morrison, M., & Schonbaum, G. R. (1976) *Annu. Rev. Biochem. 45*, 861–888.
Murata, K., Panicucci, R., Gopinath, E., & Bruice, T. C. (1990) *J. Am. Chem. Soc. 112*, 6072–6083.
Murthy, M. R. N., Reid, T. J., III, Sicignano, A., Tanaka, N., & Rossmann, M. G. (1981) *J. Mol. Biol. 152*, 465–499.
Nagai, K., & Thøgersen, C. (1984) *Nature 309*, 810–812.
Nagai, K., Hori, H., Morimoto, H., Hayashi, A., & Taketa, F. (1979) *Biochemistry 18*, 1304–1308.
Nagai, K., Kagimoto, T., Hayashi, A., Taketa, F., & Kitagawa, T. (1983) *Biochemistry 22*, 1305–1311.
Nagai, M., Yoneyama, Y., & Kitagawa, T. (1989) *Biochemistry 28*, 2418–2422.
Ogoshi, H., Sugimoto, H., & Yoshida, Z. (1975) *Tetrahedron Lett. 27*, 2289–2292.
Ortiz de Montellano, P. R. (1986) *Cytochrome P-450: Structure, Mechanism, and Biochemistry*, Plenum Press, New York.
Ortiz de Montellano, P. R., & Catalano, C. E. (1985) *J. Biol. Chem. 260*, 9265–9271.
Ozaki, Y., Kitagawa, T., Kyogoku, Y., Shimada, H., Iizuka, T., & Ishimura, Y. (1976) *J. Biochem. 80*, 1447–1451.
Ozaki, Y., Kitagawa, T., Kyogoku, Y., Imai, Y., Hashimoto-Yutsudo, C., & Sato, R. (1978) *Biochemistry 17*, 5826–5831.
Palcic, M. M., Rutter, R., Araiso, T., Hager, L. P., & Dunford, H. B. (1980) *Biochem. Biophys. Res. Commun. 94*, 1123–1127.
Palmer, G. (1979) in *The Porphyrins* (Dolphin, D., Ed.) Vol. 6, p 328, Academic Press, New York.
Peisach, J. (1975) *Ann. N.Y. Acad. Sci. 244*, 187.
Peisach, J., & Blumberg, W. E. (1970) *Proc. Natl. Acad. Sci. U.S.A. 67*, 172–179.
Peisach, J., & Gersonde, K. (1977) *Biochemistry 16*, 2539–2545.
Peisach, J., Blumberg, W. E., Ogawa, S., Rachmileintz, E. A., & Oltzik, K. (1971) *J. Biol. Chem. 246*, 3342–3355.
Penner-Hahn, J. E., McMurry, T. J., Renner, M., Latos-Grazynsky, L., Elbe, K. S., Davis, I. M., Balch, A. L., Groves, J. T., Dawson, J. R., & Hodgson, K. O. (1983) *J. Biol. Chem. 258*, 12761–12764.
Poulos, T. L., & Kraut, J. (1980) *J. Biol. Chem. 255*, 8199–8205.
Poulos, T. L., Finzel, B. C., Gunsalus, I. C., Wagner, G. C., & Kraut, J. (1985) *J. Biol. Chem. 260*, 16122–16130.
Ramsden, J., & Spiro, T. G. (1989) *Biochemistry 28*, 3125–3128.
Rein, H., Ristau, O., Hachenberger, F., & Jung, F. (1968) *Biochim. Biophys. Acta 167*, 538–546.
Remba, R. D., Champion, P. M., Fitchen, D. B., Chiang, R., & Hager, L. P. (1979) *Biochemistry 18*, 2280–2290.
Roberts, J. E., Hoffman, B. M., Rutter, R., & Hager, L. P. (1981a) *J. Am. Chem. Soc. 103*, 7656–7659.
Roberts, J. E., Hoffman, B. M., Rutter, R., & Hager, L. P. (1981b) *J. Biol. Chem. 256*, 2118–2121.
Schonbaum, G. R., & Chance, B. (1976) in *The Enzymes* (Boyer, P. D., Ed.) Vol. 13, pp 363–408, Academic Press, New York.
Schultz, C. E., Devaney, P. W., Winkler, H., DeBrunner, P. G., Chiang, R., Rutter, R., & Hager, L. P. (1979) *FEBS Lett. 103*, 102–105.
Schulz, C. E., Rutter, R., Sage, J. T., DeBrunner, P. G., & Hager, L. P. (1984) *Biochemistry 23*, 4743–4754.
Sharma, K. D., Anderson, L. A., Loehr, T. M., Terner, J., & Goff, H. M. (1989) *J. Biol. Chem. 264*, 12772–12779.
Shimizu, T., Kitagawa, T., Mitani, F., Iizuka, T., & Ishimura, Y. (1981) *Biochim. Biophys. Acta 670*, 236–242.
Spiro, T. G. (1983) in *Iron Porphyrins* (Lever, A. B. P., & Gray, H. B., Eds.) Part II, pp 89–159, Addison-Wiley, Reading, MA.
Spiro, T. G., & Burke, J. M. (1976) *J. Am. Chem. Soc. 98*, 5482–5489.
Spiro, T. G., Stong, J. D., & Stein, P. (1979) *J. Am. Chem. Soc. 101*, 2648–2655.
Springer, B. A., & Sligar, S. G. (1987) *Proc. Natl. Acad. Sci. U.S.A. 84*, 8961–8965.
Szabo, A., & Perutz, M. F. (1976) *Biochemistry 15*, 4427–4428.
Takano, T. (1977) *J. Mol. Biol. 110*, 537–568.
Teraoka, J., & Kiatagawa, T. (1980) *J. Phys. Chem. 84*, 1928–1935.
Torii, K., & Ogura, Y. (1968) *J. Biochem. 64*, 171–179.
Tsai, R., Yu, C. A., Gunsalus, I. C., Peisach, J., Blumberg, W., Orme-Johnson, W. H., & Beinert, H. (1970) *Proc. Natl. Acad. Sci. U.S.A. 66*, 1157–1163.
Tsubaki, M., Srivatsa, R. B., & Yu, N.-T. (1982) *Biochemistry 21*, 1132–1144.
Varadarajan, R., Szabo, A., & Boxer, S. G. (1985) *Proc. Natl. Acad. Sci. U.S.A. 82*, 5681–5684.
Varadarajan, R., Lambright, D. G., & Boxer, S. G. (1989a) *Biochemistry 28*, 3771–3781.
Varadarajan, R., Zewert, T. E., Gray, H. B., & Boxer, S. G. (1989b) *Science 243*, 69–72.
White, R. E., & Coon, M. J. (1980) *Annu. Rev. Biochem. 49*, 315.
White, R. E., Sligar, S. G., & Coon, M. J. (1980) *J. Biol. Chem. 255*, 11108–11111.
William-Smith, D. L., & Morrison, P. J. (1975) *Biochim. Biophys. Acta 405*, 253–261.
William-Smith, D. L., & Patel, K. (1975) *Biochim. Biophys. Acta 405*, 243–252.
Williams, R. J. P. (1974) in *Iron in Biochemistry and Medicine* (Jacobs, A., & Worwood, M., Eds.) pp 183–219, Academic Press, New York.
Yamada, H., Makino, R., & Yamazaki, I. (1975) *Arch. Biochem. Biophys. 169*, 344–353.
Yamaguchi, K., Watanabe, Y., & Morishima, I. (1992) *Inorg. Chem. 31*, 156–157.
Yu, N.-T., & Kerr, E. A. (1988) in *Biological Applications of Raman Spectroscopy* (Spiro, T. G., Ed.) Vol. 3, pp 39–95, John Wiley & Sons, New York.